Section 6 – Grid connection of converter circuits

6.1 Injection of harmonics into the utility network from power electronic circuits.

Power electronic circuits inject harmonics and other noise into the utility supply network. Consider the simple diode bridge rectifier example below.

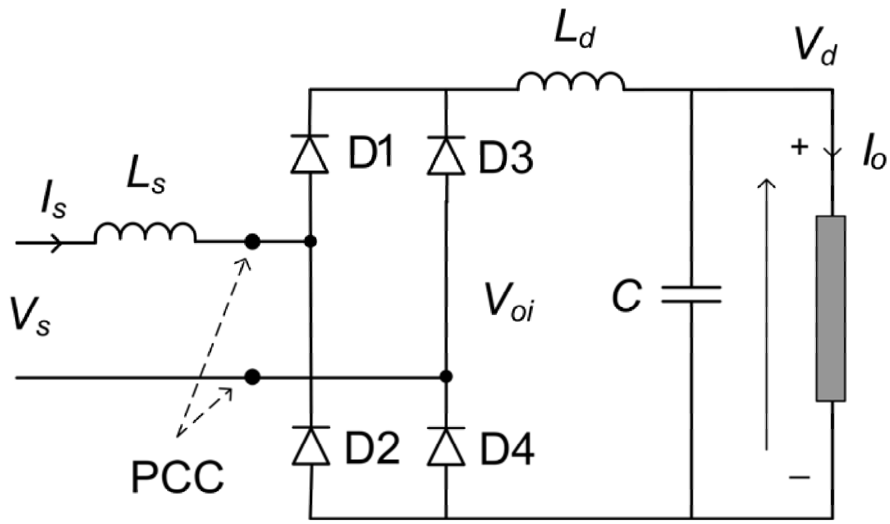

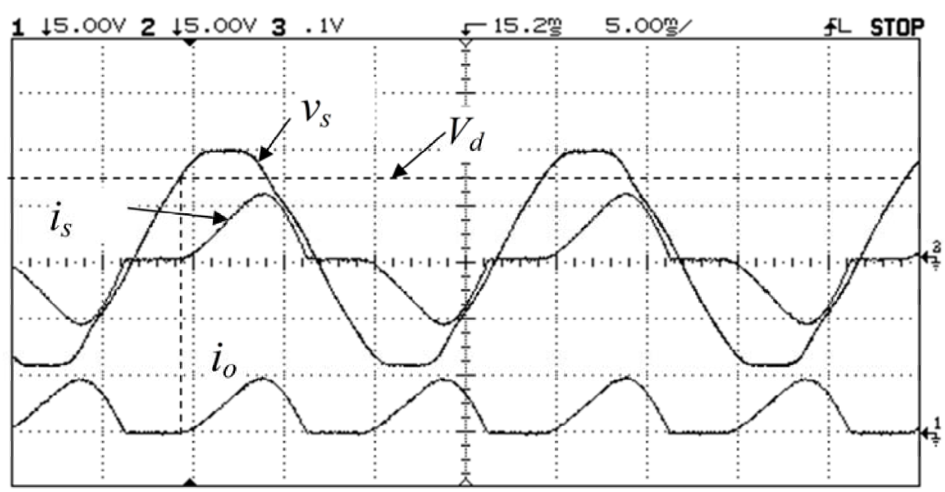

Figure 6.1

Harmonic generation on the utility AC side is given by

$$i_s = i_1 + i_h \qquad [6.1]$$

where $i_1 = I_{1\max} \sin(\omega t - \theta)$ [6.2]

$$i_h = \sum_{n=3,5,7,...}^{\infty} I_{n\max} \sin(n\omega t + \theta_n) \qquad [6.3]$$

Typical harmonic content of a single-phase rectifier with no input filter:

Table I

n	*3*	*5*	*7*	*9*	*11*	*13*	*15*	*17*
$(I_h / I_1)\%$	73.2	36.6	8.1	5.7	4.1	2.9	0.8	0.4

The input harmonic currents cause voltage distortion in the AC voltage at the Point of Common Coupling (PCC, where other loads are connected to the AC supply lines). This is given by

$$V_h = n\omega L_s I_h \qquad [6.4]$$

where L_s is the source impedance behind AC source at the PCC (see Figure 6.2). Note that the AC source impedance is normally highly inductive. The voltage at the PCC is given by

$$V_{PCC} = V_s \angle 0^0 - \sum_{n=3}^{\infty} jn\omega L_s \times I_h \angle \theta_n \qquad [6.5]$$

which has higher order terms.

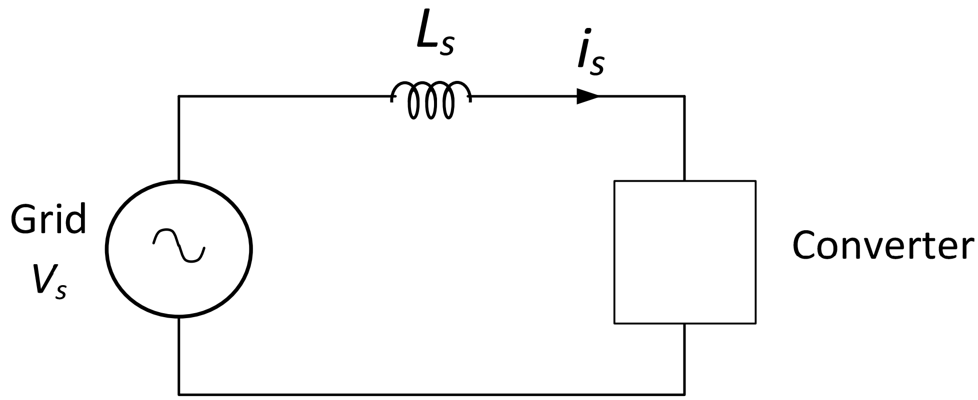

Figure 6.2

The distorted AC voltage at the PCC, where other loads may be connected, can be undesirable for these other users. It is also undesirable for the utility authorities because penetration of harmonics into the AC network can cause other problems.

When distributed single-phase power converters, such as in figure 3, are operated from line-neutral voltages of a three-phase supply network supply, the third and its multiple order harmonic currents become co-phasal. The harmonic load (or neutral) currents are

$$i_{ah} = I_{n\max} \sin\left\{n\omega t - \theta_n\right\}$$

$$i_{bh} = I_{n\max} \sin\left\{n\left(\omega t - 120^{\circ}\right) - \theta_n\right\} \qquad [6.6]$$

$$i_{ch} = I_{n\max} \sin\left\{n\left(\omega t - 240^{\circ}\right) - \theta_n\right\}$$

Note that fundamental neutral currents of the three phases add up to zero for balanced loads. However, for n = 3, 6, 9,… , the neutral wire currents of such harmonic orders for each rectifier are in-phase and therefore add up algebraically in the composite neutral wire to which the neutral wires of individual phases connect. [Note that $sin(n\omega t - n\times 120°) = sin(n\omega t)$ for $n = 3, 6, 9,\ldots$]. For n = 3, the composite neutral wire current is given by

$$i_3 = I_{3\max} \sin\left(3\omega t - \phi_3\right) + I_{3\max} \sin\left(3\left(\omega t - 120°\right) - \theta_3\right) +$$

$$I_{3\max} \sin\left(3\left(\omega t - 240°\right) - \theta_3\right)$$

$$= 3I_{3\max} \sin\left(3\omega t - \theta_3\right). \qquad [6.7]$$

The neutral-wire current is thus given by

$$i(h) = \sum_{n=3,6,9,\ldots}^{\infty} 3I_{h\max} \sin\left(3\omega t - \phi_h\right) \qquad [6.8]$$

The algebraic addition of all third and its multiple order harmonic currents may lead to unacceptably large current in the composite neutral wire of three-phase system where the neutral wires are connected together as indicated in Figure 6.3. Note that the lower order harmonics in AC the input current of a single-phase rectifier are for n = 3, 5, 7, 9, 11… and so on.

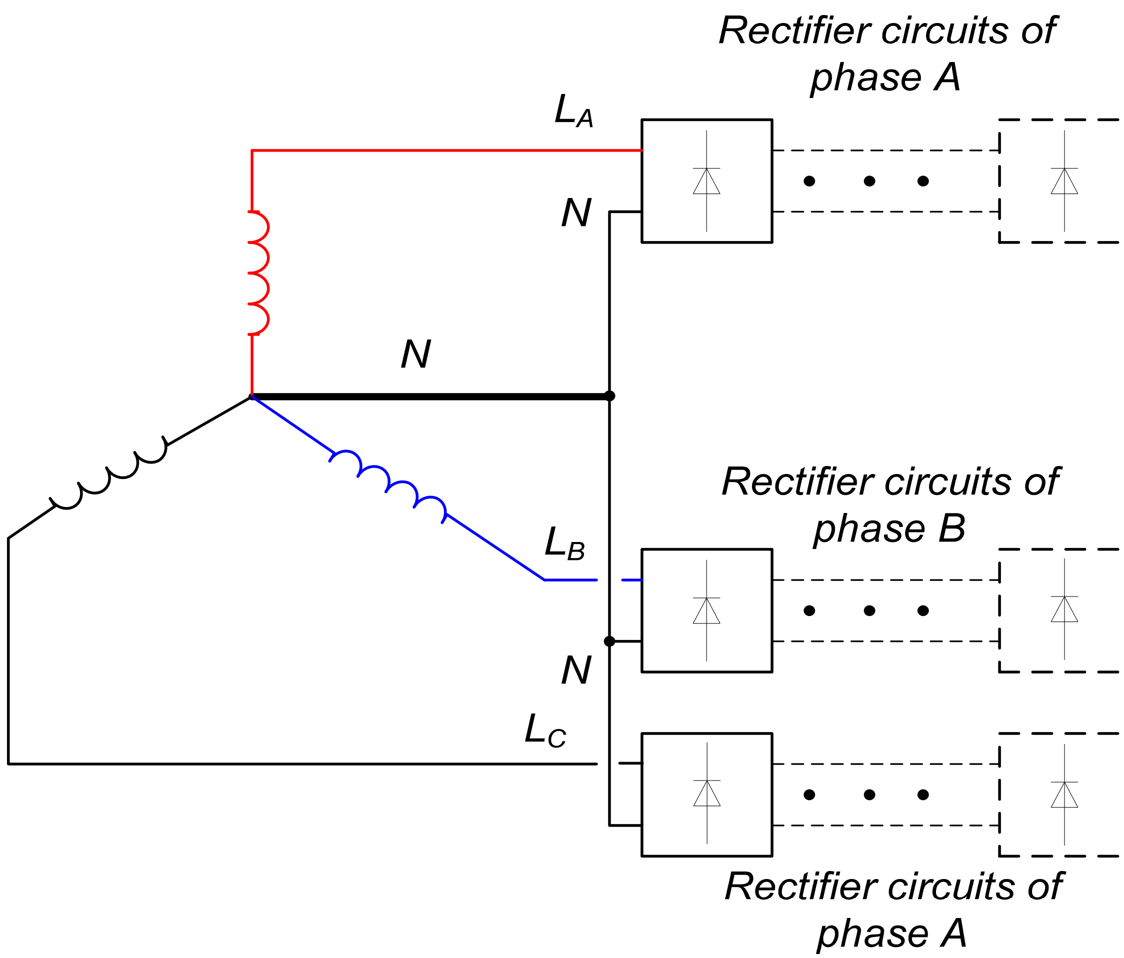

Figure 6.3

Power electronic converter circuits also cause some phase angle of lag between the input voltage and the fundamental input current I_1, resulting in less than unity *displacement factor* and hence low *power factor*. Note that operation of converter circuit-load with lower than unity power factor may mean exhaustion of the AC supply current capacity before full load (in kW) capacity is reached.

Note also that increasing the pulse number of the rectifier to 6, 12, 24, and so on brings the waveform of the input AC current closer to sinusoidal; however, it does not improve phase lag of input current of the converter. In any case, rectifiers with high pulse number (greater than 6) can only be justifiable (from cost considerations) for high power load. For low and medium power applications, PWM rectifier techniques are now used.

6.1.1 Harmonic and power factor standards:

The harmonic content of Table I is usually not acceptable to utility providers. The IEC61000 standard stipulates the acceptable input current harmonics in many countries. In order to mitigate the input harmonic and power factor issues, standards which stipulate the maximum harmonic current envelope for specified harmonics that can be injected into the utility grid exist. Standards in terms of minimum power factor of a load (which may include power converters) are also in use in many countries. Consequently, OEM product suppliers are required to comply with these standards.

Rectifier circuits for many low to medium power equipment now-a-days tend to avoid an input 50Hz transformer from size, weight and cost considerations. In other words, direct rectification from the AC supply, followed by appropriate converter circuits that produce the required DC output voltage for the load concerned is preferred. These rectifier circuits also include facilities that force the input AC current to be 50 Hz sinusoidal and in-phase with the AC input voltage.

For grid requirements for PVS, more can be found in Chapter 3, Textbook 3. For grid requirements for WTS see Chapter 7, Textbook 3.

6.2 Single-phase, active front-end (PWM) rectifier (unidirectional)

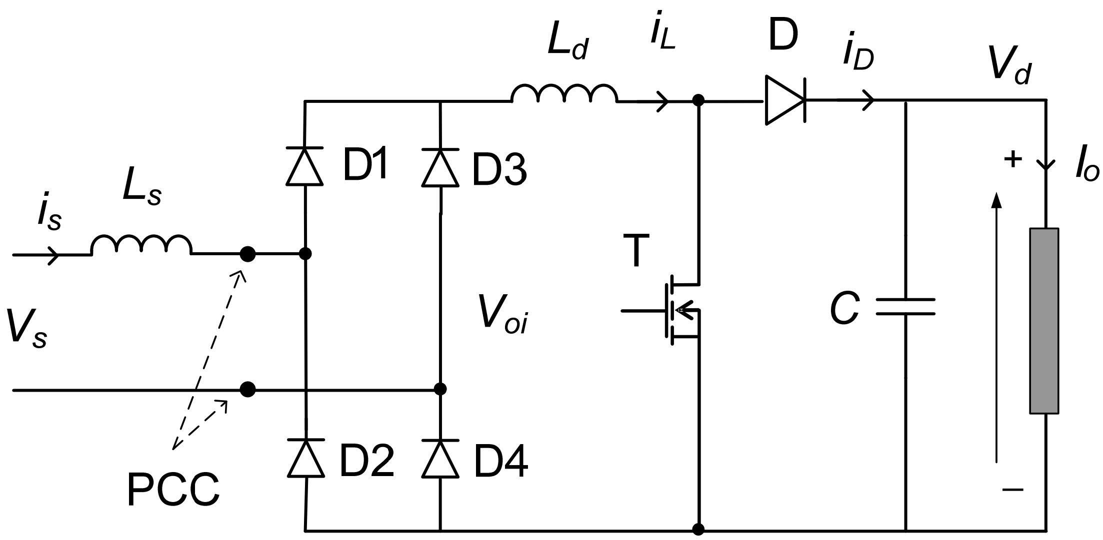

Figure 6.4

This rectifier employs a single-switch boost stage at the output of the diode-bridge rectifier. It forces the input current waveform to be sinusoidal and be in-phase with the input AC voltage waveform. The boost inductor current is made continuous over each switching period in each AC half-cycle. The switching frequency of the switch T is often much higher than the utility AC frequency (50 or 60 Hz). Moreover, the inductor current is forced to become sinusoidal over the each half-cycle of the AC supply. For this, the duty cycle *D* of the switch T must be an inverse of the rectified sine wave. Because of boost mode operation, the output DC voltage V_d must be higher than the peak of the supply voltage by a reasonable margin, i.e.,

$$V_d > V_{PCC,max} \tag{6.9}$$

The AC source inductance L_s and L_d together is the boost inductance. With sufficiently high switching frequency, f_s, additional inductance L_d may not be required.

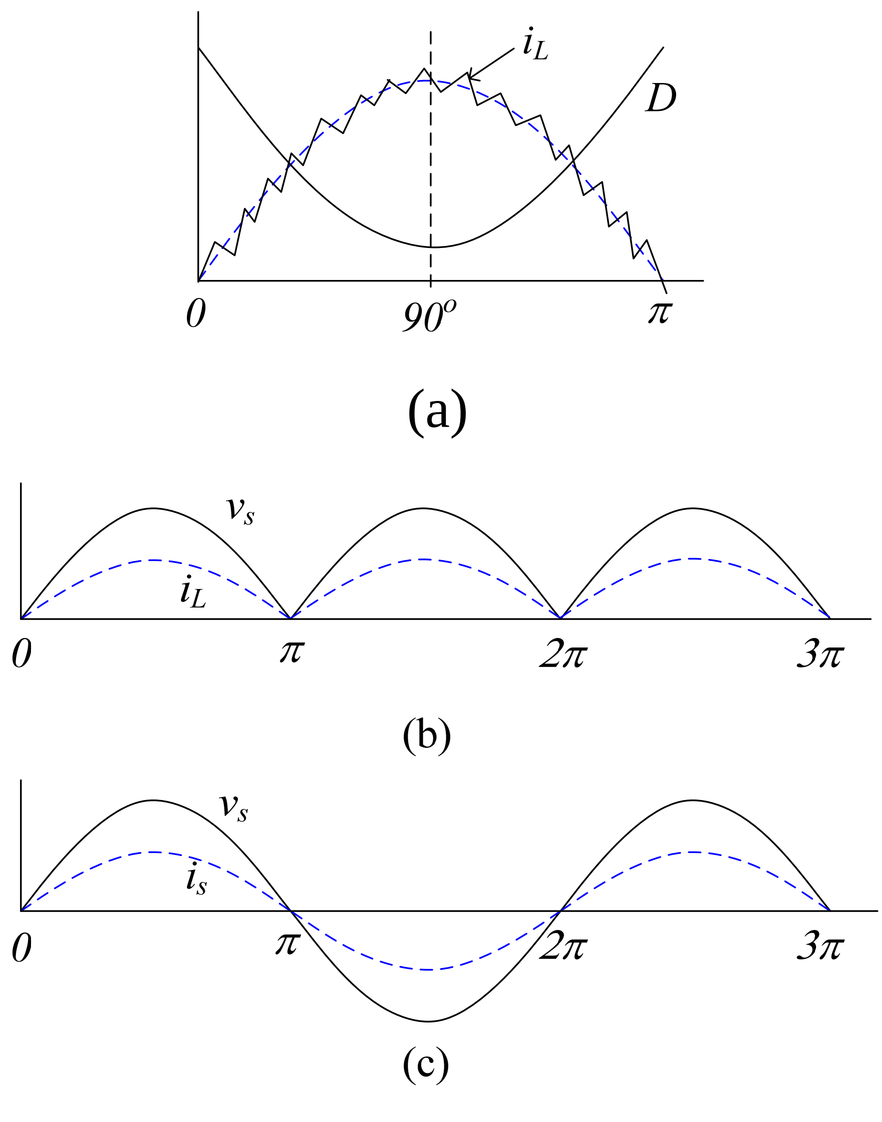

Figure 6.5

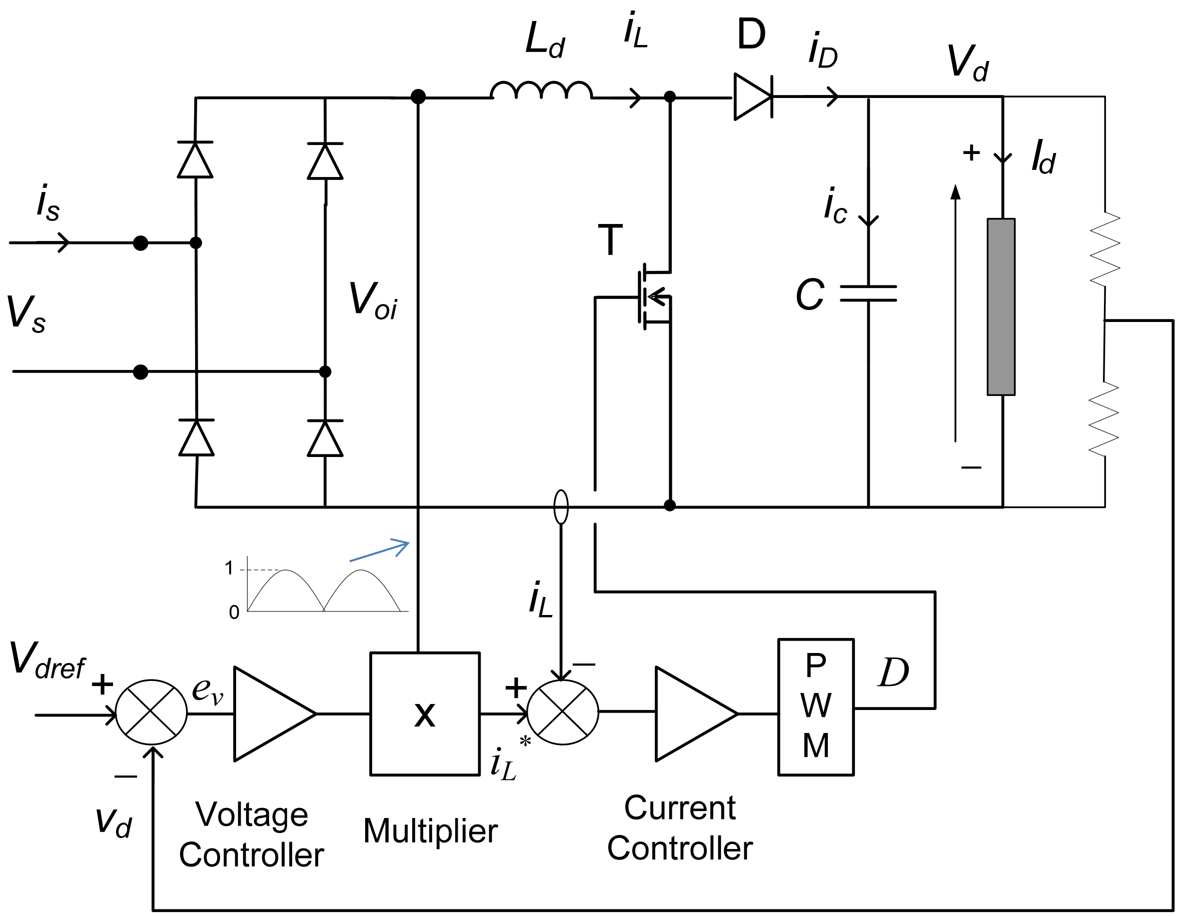

Figure 6.6

Figure 6.6 shows the control structure for such a PWM rectifier. The outer voltage loop error is amplified by a voltage controller and then multiplied by a unit amplitude signal which reflects the diode rectifier output voltage. The multiplier output is a variable amplitude rectified sine wave which acts as the inductor current reference. The current control loop ensures rectified sinewave current i_L through the boost inductor (i_L is also the output of the rectifier). The diode bridge unfolds this current on the AC side, so that the input current i_s is sinusoidal

AC and in phase with v_s. The output of the current controller produces a variable duty cycle D, via a pulse-width modulator or a comparator with a hysteresis band. This results in the input current which is sinusoidal (except for the PWM ripple) and in-phase with V_s. The PWM ripple is negligible when a high PWM switching frequency or a small hysteresis band is used.

In the following analysis we will assume that the output voltage V_d remains constant during a switching period T and that the AC input current is a perfect sinusoid and in-phase with V_s. Thus,

$$v_s = V_{s\max} \sin \omega t \qquad [6.10]$$

$$i_s = I_{s\max} \sin \omega t \qquad [6.11]$$

$$p_{in} = v_s \times i_s = V_s I_s + V_s I_s \cos 2\omega t = V_d I_d \qquad [6.12]$$

where V_s and I_s are RMS values.

$$I_d = \frac{V_s I_s}{V_d} \qquad [6.13]$$

Assuming that the AC input voltage v_s and the output voltage V_d remain constant during a switching period T,

$$\Delta I_L = \frac{v_s}{L_d} t_{on} \qquad [6.14]$$

$$t_{on} = \frac{L_d \Delta I_L}{|v_s|} \qquad [6.15]$$

assuming negligible L_s.
With a PWM current controller, the switching period T_s is constant, and $t_{on} = DT_s$. Thus

$$D = \frac{L_d f_s \Delta I_L}{|v_s|} \qquad [6.16]$$

which implies that the duty cycle D varies inversely with the value of the AC supply, during a PWM cycle, as indicated in Fig 6.5(a).

Assuming that D = 0.5 when $|v_s| = \frac{V_{s,\max}}{2}$;

$$f_s \Delta I_L = \frac{V_{s,\max}}{4L_d} \qquad [6.17]$$

L_d is selected from the desirable ripple current Δi_L using (6.17). The value of L_d found from (6.17) is the total supply circuit inductance, which includes the source inductance L_s.

Assuming that V_d is constant, which implies that capacitor C does not carry any DC current,

$$i_c = \frac{V_s I_s}{V_d}\cos 2\omega t \qquad [6.18]$$

The voltage ripple in the capacitor voltage is then approximated as

$$\Delta V_d = \frac{1}{C}\int_0^{T/4} \frac{V_s I_s}{V_d}\cos 2\omega t dt = \frac{1}{C}\frac{V_s I_s}{2\omega V_d} = \frac{I_d}{2\omega C} \qquad [6.19]$$

Note that the switching ripple current, which has been neglected in this analysis, also flows through the capacitor. Note also that while the boost inductor L_d is selected from an acceptable switching ripple and the switching frequency, the output capacitor C must be selected using the maximum load current and supply frequency ω which is normally much lower than the switching frequency.

The switch and diode current waveforms both consist of pulses which have amplitude and width both varying sinusoidally. DC and RMS current calculations for the switch and the diode will not be included in this course.

6.2.1 Three-phase, active front-end PWM rectifier (unidirectional)

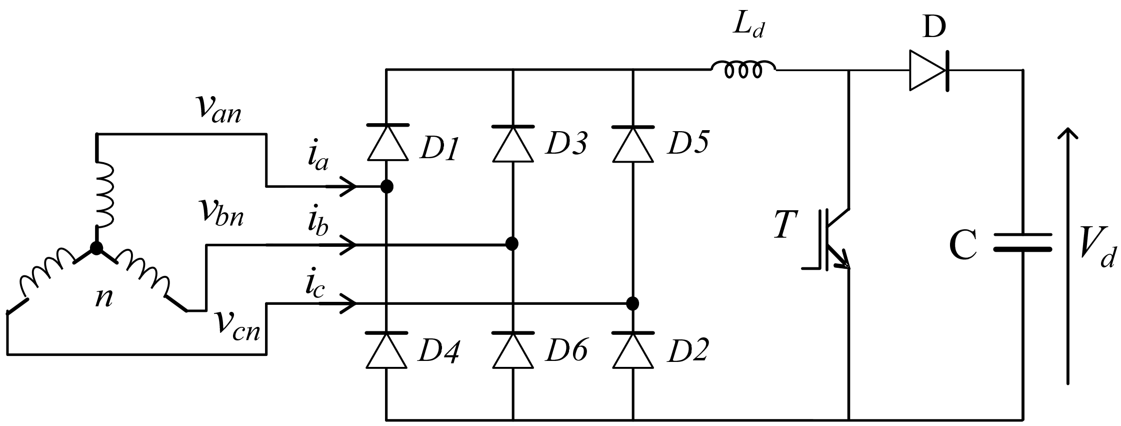

Figure 6.7 Single-switch front-end three-phase rectifier.

The control system for this rectifier is similar to the one indicated in Figure 6.6. It should be noted that power flow of circuits 6.4 and 6.7 is unidirectional.

The simple controller arrangement of Figures 6.5 does not lend easily to control of active and reactive powers. A more general approach using converters for bidirectional power flow and axes transformations of voltages and currents to quadrature $\alpha\beta$ and dq reference frames will be discussed in a latter section.

6.2.2 Single-phase converter for bi-directional power flow

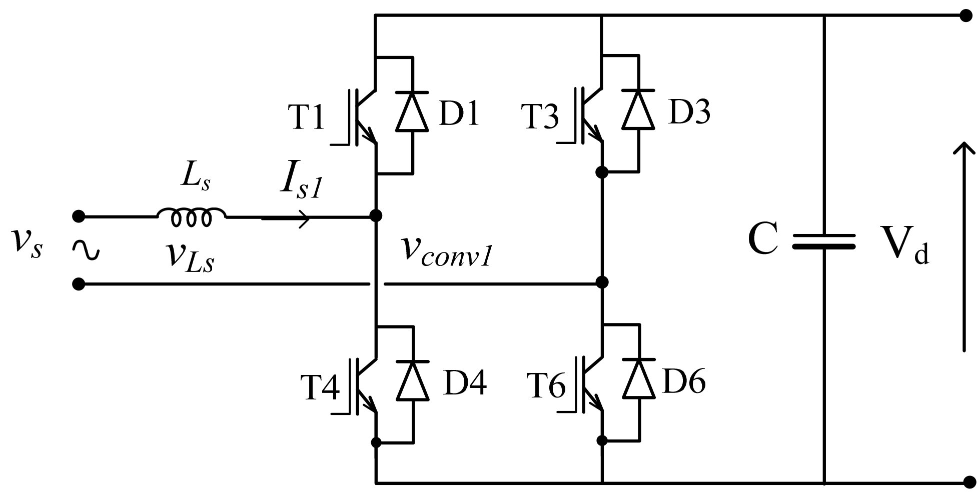

Figure 6.8

This rectifier is capable of rectifying the AC supply into DC and vice versa, giving bi-directional power flow. The current waveform in the AC side can be sinusoidal and in- phase with the AC supply when rectifying or inverting. Any arbitrary phase angle between the AC source and the AC voltage produced by the inverter can also be set via current (mode) control of the inverter. The control structure for this rectifier/inverter can use linear control laws rather than the non-linear controller indicated in Figure 6.6, using the instantaneous *pq* theory.

Note that the converter operates in the boost mode when rectifying and in buck mode when inverting. Thus,

$$V_d > V_{s,\max} \qquad [6.20]$$

for both modes of operation. V_d is maintained constant at a value which is higher than the peak of the AC supply voltage, $V_{s,max}$.

Rectifier operation:

$$P = V_d I_d = V_s I_s \cos\phi \qquad [6.21]$$

The angle between the input AC voltage and current can be arbitrarily set at any angle ϕ. Note that $\phi = 0$ is preferred of course.

6.2.3 Inverter connection to grid and control

Single-phase converter for bi-directional power flow

It can be shown that when two sinusoidal AC supplies of the same frequency are connected to each other, the power transfer across the two systems is given by

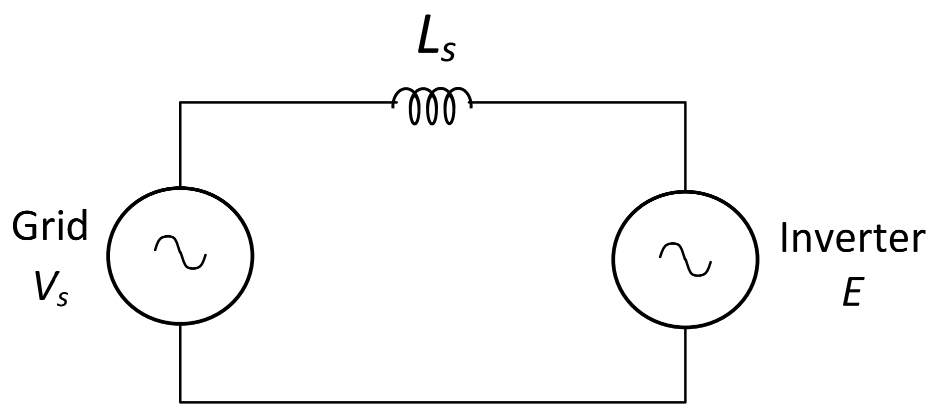

Figure 6.9

$$P = \frac{V_s E}{X_s} \sin\delta \qquad [6.22]$$

where $E = mV_d/\sqrt{2}$ is the RMS value of converter output produced (on the AC side) when operating as an inverter. m is the depth of modulation for the SPWM inverter and V_d is the DC supply voltage to the inverter.

δ is the (load) angle in radians. This is the angle between the grid-side AC and inverter output AC phasors.

and X_s is the reactance ωL_s; $\omega = 2\pi f$ is the supply frequency in rad/sec.

Note that equation 6.22 is covered in UNSW EET courses ELEC3105 and ELEC4611 in the section on synchronous machines operating as generators connected to the AC grid.

From Figure 6.9,

$$v_s = v_{conv1} + v_{Ls} \tag{6.23}$$

In terms of phasor quantities,

$$V_s = V_{conv1} + V_{Ls} \tag{6.24}$$

$$V_{Ls} = j\omega L_s I_1 \tag{6.25}$$

where subscript 1 indicates fundamental quantities.

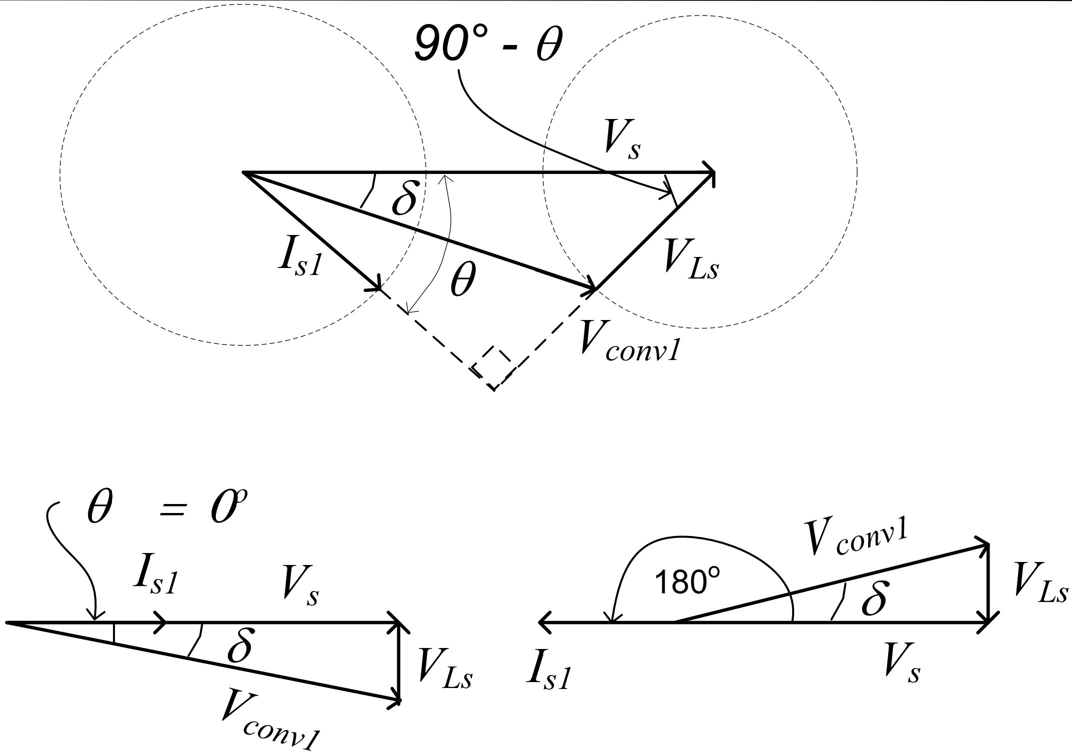

(a) Rectification (b) Inversion

Figure 6.10 (a) Rectification with UPF (b) Inversion with UPF

From [6.22]

$$P = V_s I_{s1} \cos\theta = \frac{V_s V_{conv1} \sin\delta}{\omega L_s} \tag{6.26}$$

$$\omega L_s I_{s1} \cos\theta = V_{Ls} \cos\theta = V_{conv1} \sin\delta .$$

The reactive power supplied by the AC source is given by

$$Q = V_s I_{s1} \sin\theta = \frac{V_s^2}{\omega L_s}\left(1 - \frac{V_{conv1}}{V_s}\cos\delta\right) \qquad (6.27)$$

since $V_s - \omega L_s I_{s1} \sin\theta = V_{conv1} \cos\delta$

Q is the sum of the reactive powers absorbed by the converter and the inductance L_s.

Note that the desired values of P and Q can be obtained by controlling the magnitude and phase of V_{conv1}. More appropriately, P and Q can be controlled by controlling I_{s1} and θ directly. Note also that equations 6.26 and 6.27 apply only to steady-state conditions.

Three-phase converter for bi-directional power flow

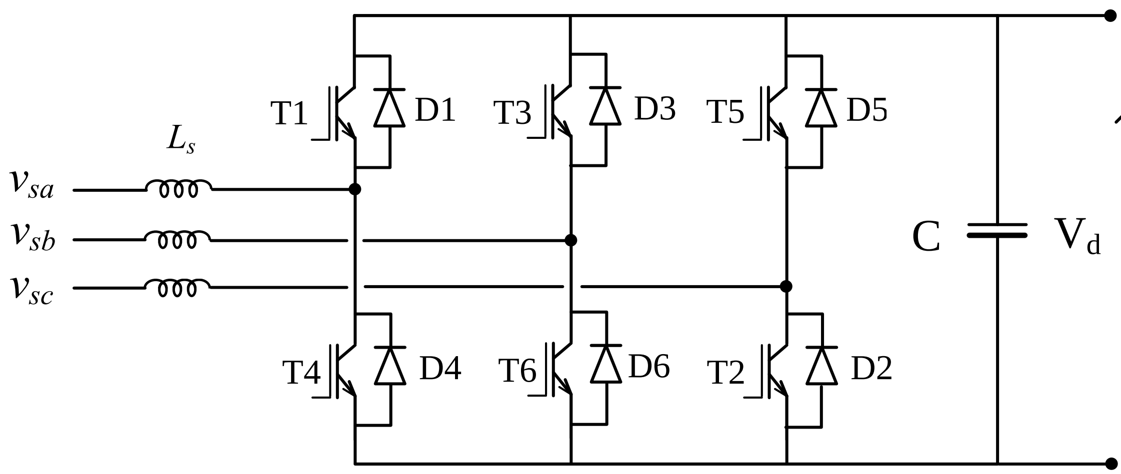

Figure 6.11 Bi-directional AC-DC converters.

This is the three-phase version of the bi-directional rectifier/inverter of the previous section. As previously,

$$V_d > V_{s,\max l-l} \qquad [6.28]$$

Comments on the single-phase bi-directional rectifier/inverter and equations [6.22-27] apply equally well here, except that

$$P = V_d I_d = 3V_s I_s \cos\theta \quad \text{for rectifier operation} [6.29]$$

where V_s and I_s are in per-phase RMS values. V_d is maintained constant by closed loop control.

$$P = \frac{3V_s E}{X_s}\sin\delta \quad \text{for inverter operation} \qquad [6.30]$$

where V_s and E ($= 0.354 m V_d$) are in per-phase RMS values. The analyses of active and reactive power flows, P and Q, when a three-phase SPWM inverter is connected to a three-phase grid is the same as in previous pages when carried out in per-phase. The instantaneous *pq* theory simplifies controller designs for this, as will be shown in a latter section.

AC-AC conversion.

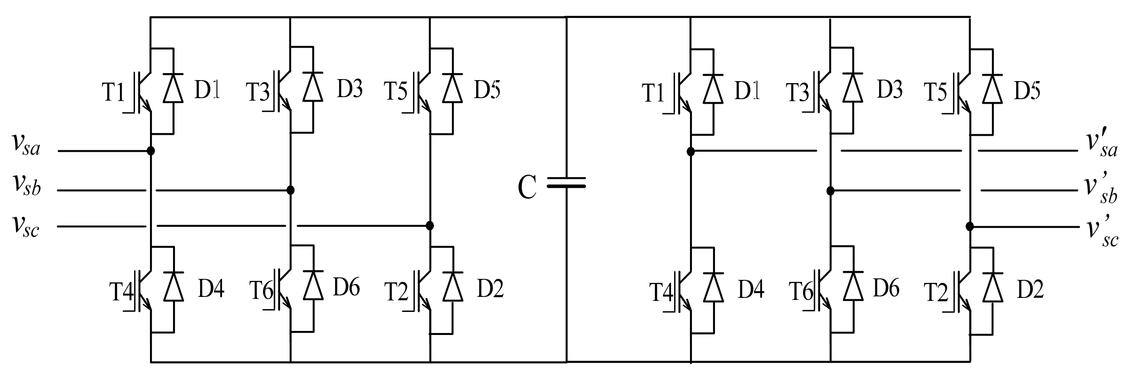

Figure 6.12 Bi-directional boost rectifier-inverter used in wind energy systems.

6.3 Grid synchronization of converters (*This section is covered from Textbook 3, Chapter 4.)*

V and f are grid variables. These change continuously due to:

- transient variations of loads at the point of common coupling (PCC)
- harmonics drawn or injected into the grid at the PCC
- when the power injected into or drawn from the grid is comparable to the rating of the grid
- when abnormal operating conditions occur, such as sudden change of load, lightning, islanding and so on.

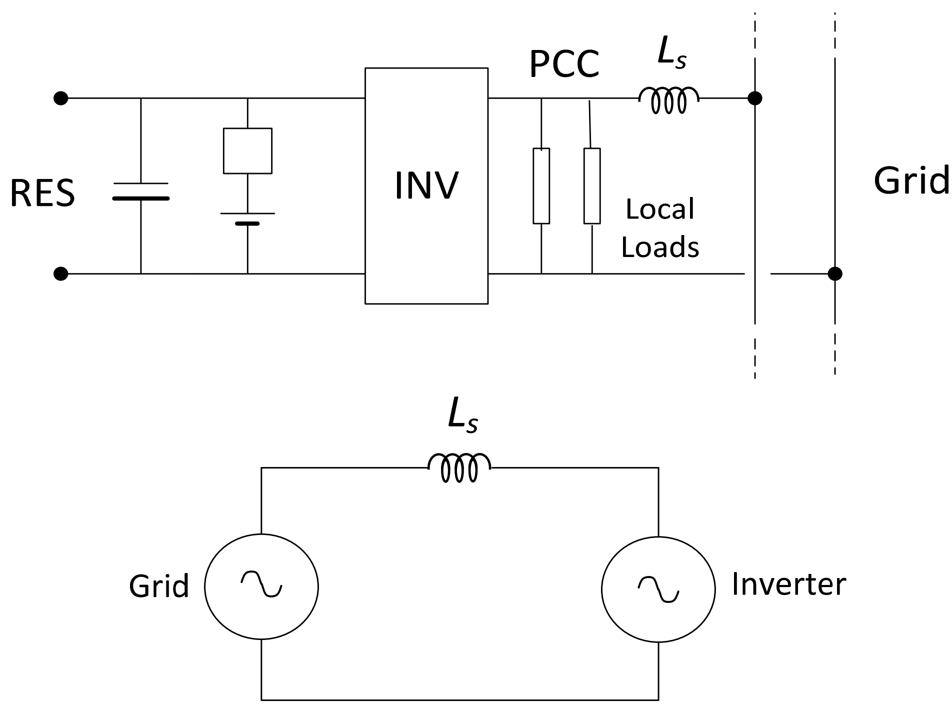

Figure 6.13

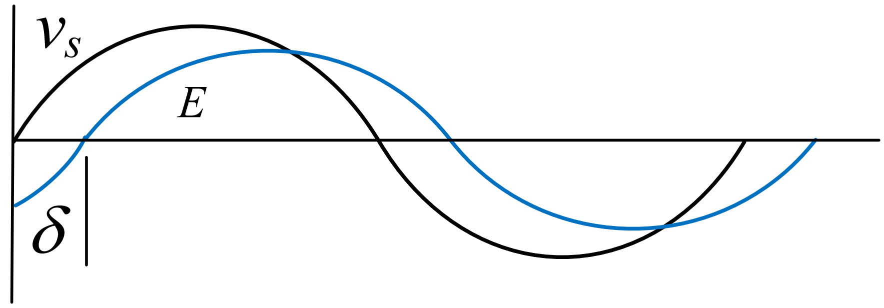

Figure 6.14

Power flow between inverter I and grid G depends on the voltage, phase angle δ, frequency and the series inductance L_s. Sustained frequency mismatch can lead to excessive phase angle to develop between I and G, leading to excessive or disastrous power flow in either direction (depending on the phase angle). There are strict codes which disconnect the sources when voltage, current and frequency are outside permissible limits.

Thus, the grid must be continuously and precisely monitored. Note that inverters can change their voltage, frequency and δ angle very fast (in msecs) compared to minutes for large rotating generators. Phase-locked loops (PLLs) of various complexities are available for monitoring the grid voltage, its frequency and instantaneous angle θ.

6.3.1 Grid Synchronization using PLLs

The Basic PLL

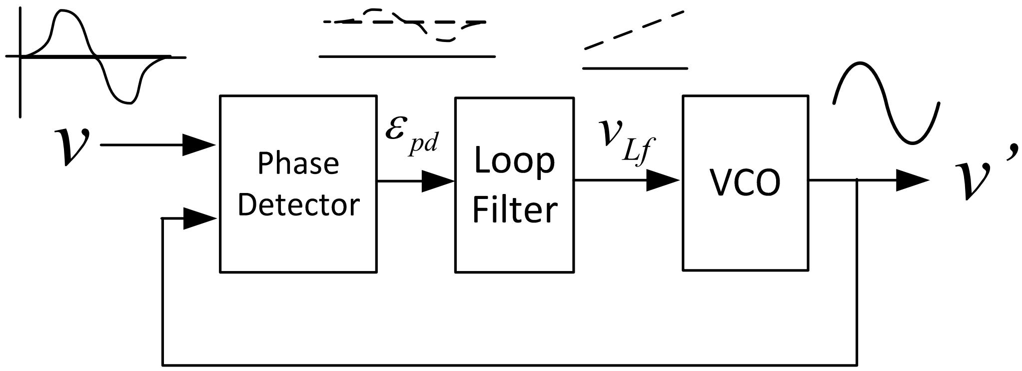

Figure 6.15

$$v = V\sin\theta = V\sin\left(\omega t + \phi\right) \tag{6.31}$$

$$v' = \cos\theta' = \cos\left(\omega' t + \phi'\right) \tag{6.32}$$

$$\begin{aligned}\varepsilon_{pd} &= VK_{pd}\sin\left(\omega t + \phi\right) * \cos\left(\omega' t + \phi'\right) \\ &= \frac{VK_{pd}}{2}\begin{bmatrix}\sin\left(\left(\omega - \omega'\right)t + \left(\phi - \phi'\right)\right) \\ +\sin\left(\omega + \omega'\right)t + \left(\phi + \phi'\right)\right)\end{bmatrix}\end{aligned} \tag{6.33}$$

Assume that the $(\omega + \omega')$ frequency part is filtered by the loop filter adequately, so that

$$v_{Lf} = \frac{VK_{pd}}{2}\left[\sin\left(\left(\omega - \omega'\right)t + \left(\phi - \phi'\right)\right)\right] \tag{6.34}$$

When the voltage controlled oscillator (VCO) output frequency ω' becomes close to ω, (using some feed-forward method) and loop gain, i.e., when $\omega \approx \omega'$,

$$v_{Lf} = \frac{VK_{pd}}{2}\sin\left(\phi - \phi'\right) \tag{6.35}$$

When the phase error is small, i.e., the PLL is well locked,

$$v_{Lf} = \frac{VK_{pd}}{2}\left(\phi - \phi'\right) = \frac{VK_{pd}}{2}\left(\theta - \theta'\right) \tag{6.36}$$

The averaged VCO frequency,

$$\omega' = \left(\omega_c + \Delta\overline{\omega}'\right) = \left(\omega_c + K_{vco}\overline{v}_{Lf}\right)$$

$$\overline{\omega}' = K_{vco}\overline{v}_{Lf}$$

$$\overline{\theta}'(t) = \int \overline{\omega}'\,dt = \int K_{vco}\overline{v}_{Lf}$$

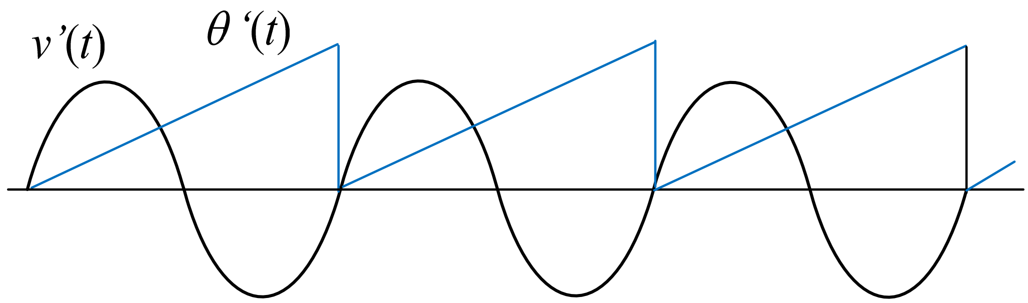

Figure 6.16

6.3.2 Linearized small signal model of a PLL

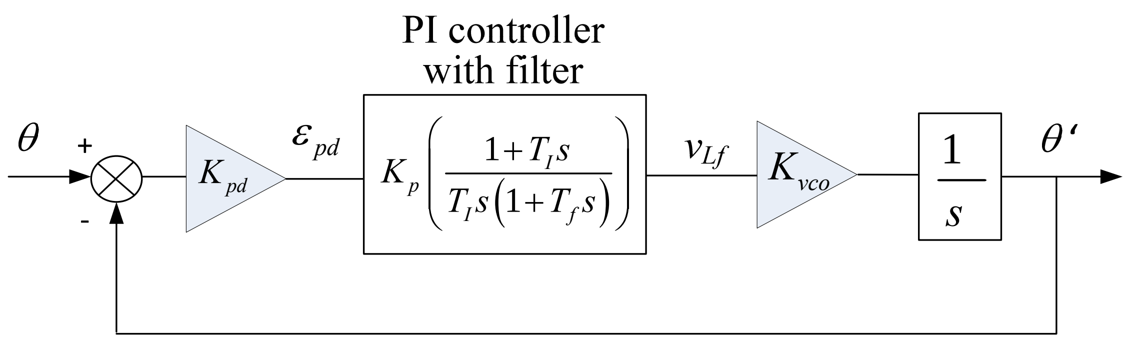

Figure 6.17

Open-loop transfer function:

$$F(s) = PD(s) * LF(s) * VCO(s) = K_{in} = \frac{K_p \left(\frac{1 + T_I s}{T_I s} \right)}{s} = \frac{K_p s + \frac{K_p}{T_I}}{s^2}$$

(6.37)

Closed-loop transfer function:

$$H(s) = \frac{G}{1-G} = \frac{K_p s + \frac{K_p}{T_I}}{s^2 + K_p s + \frac{K_p}{T_I}} \quad (6.38)$$

$$\text{Error transfer function} = E(\theta) = \frac{\varepsilon_{pd}(s)}{\theta(s)} = \frac{s^2}{s^2 + K_p s + \frac{K_p}{T_I}}$$

(6.39)

$$H(s) = \frac{2\xi\omega_n s + \omega_n^2}{s^2 + 2\xi\omega_n s + \omega_n^2} \quad (6.40)$$

$$\omega_n = \sqrt{\frac{K_p}{T_I}} \qquad \xi = \frac{\sqrt{K_p T_I}}{2} \quad (6.41)$$

6.3.3 PLL Response

Settling time to within 1% of the step change in frequency is

$$t_s = 4.6\tau \quad \text{with} \quad \tau = \frac{1}{\xi\omega_n} \quad (6.42)$$

$$K_p = 2\xi\omega_n = \frac{9.2}{t_s}; \quad T_I = \frac{2\xi}{\omega_n} = \frac{t_s \xi^2}{2.3} \quad (6.43)$$

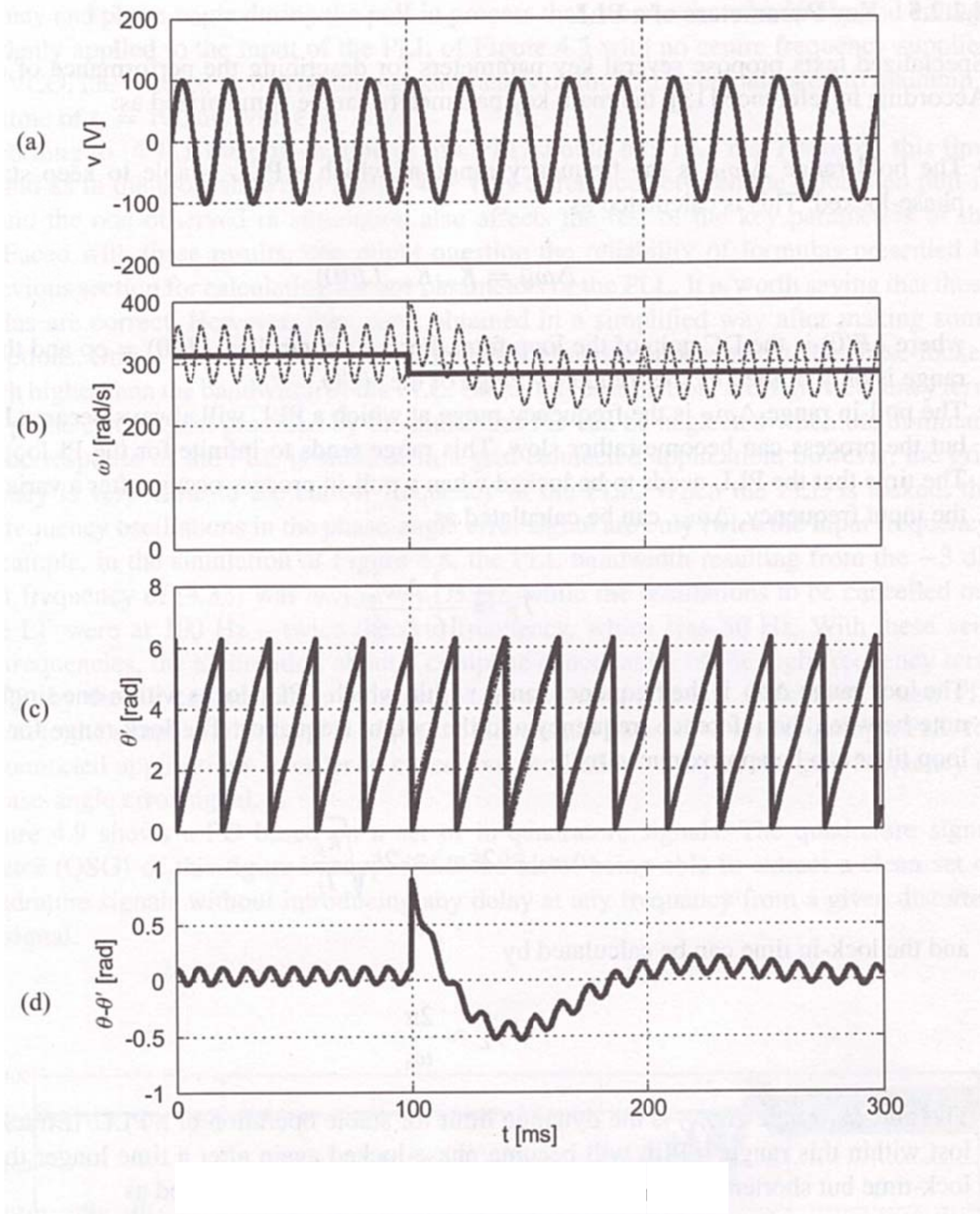

Figure 6.18 Step response of the PLL of Figure 6.17

6.3.4 Key parameters of a PLL:

1. Loop Gain: $K_{pd} K_{vco} K_{filter}$

   The DC gain of the PI controller with filter is infinitely large (= ∝) because of the pole at the origin (i.e., at s = 0). The VCO must have the frequency range within which the frequency of v_s varies.

2. The pull-in range: $\Delta\omega_{in}$

   The frequency range within which the PLL will always lock in. The time that the PLL requires to lock-in after a variation $\Delta\omega_{in}$:

$$T_P \approx \frac{\pi^2 \Delta\omega_{in}^2}{16\xi\omega_n^3} \qquad (6.44)$$

3. The lock-in range: $\Delta\omega_L$

   The frequency range within which the PLL locks within one beat between ω and ω'.

$$\Delta\omega_L \approx 2\xi\omega_n \approx 2\xi\sqrt{\frac{K_p}{T_I}} \qquad (6.45)$$

4. Lock in time: T_L

$$T_L \approx \frac{2\pi}{\omega_n} \tag{6.46}$$

5. The pull-out range: $\Delta\omega_{po}$

$$\Delta\omega_{po} \approx 1.8\omega_n\left(\xi + 1\right) \tag{6.47}$$

The pull-in process:

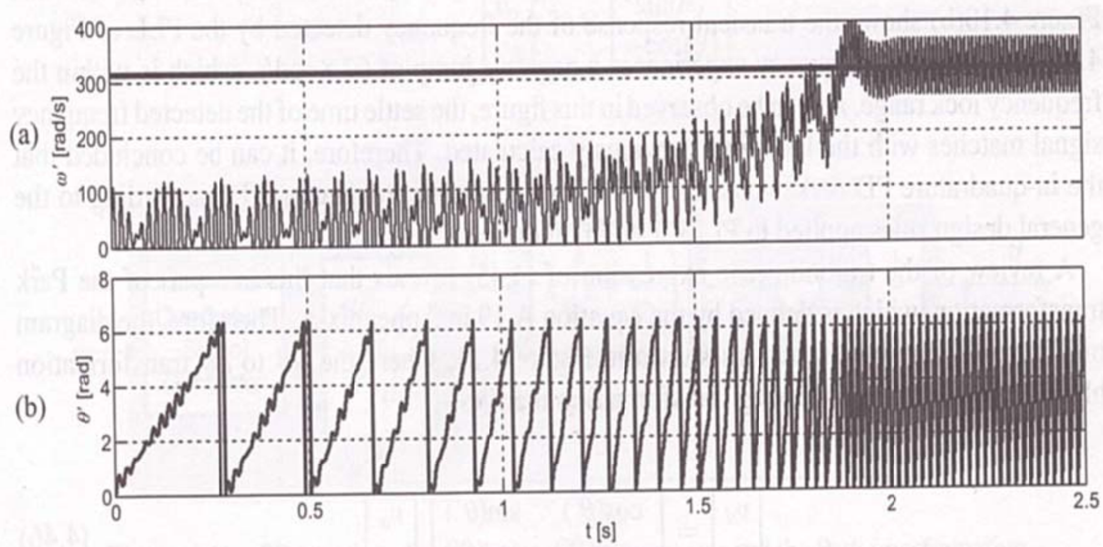

Figure 6.19

v_s is suddenly applied to the PLL

t_s = 100 msec, ξ = 0.707

The pull-in process in the basic PLL is rather long. Why?

6.3.5 PLL with in-quadrature signals

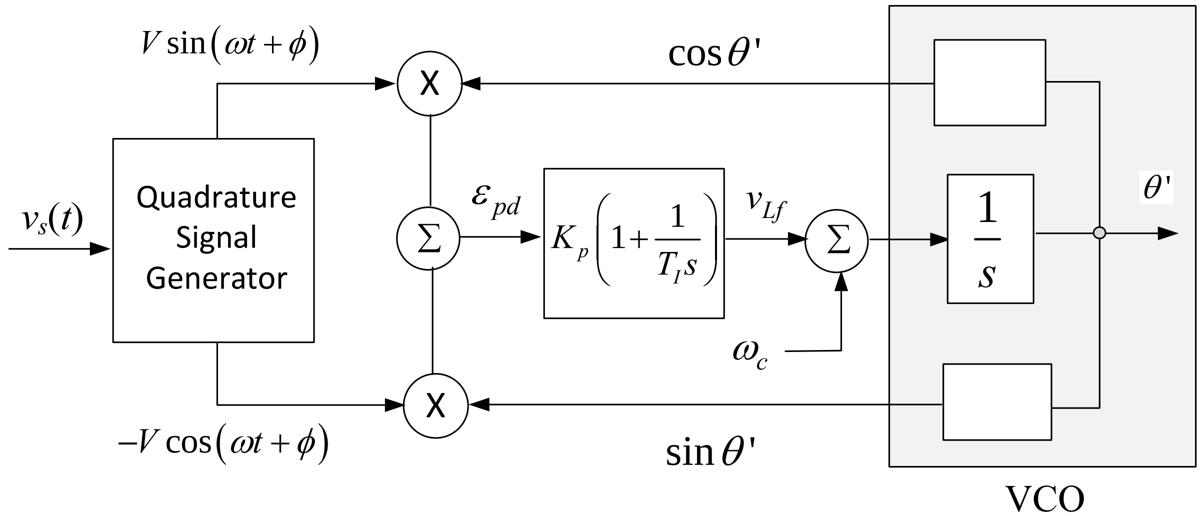

Figure 6.20

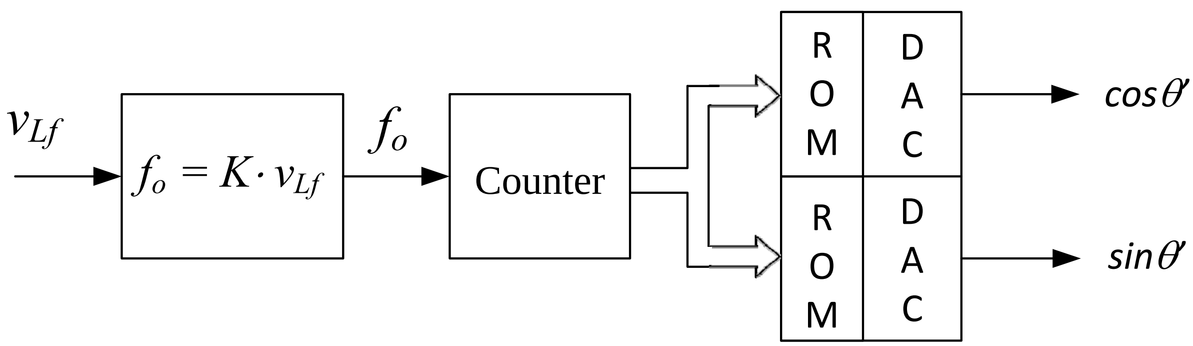

Figure 6.21

In this scheme, the grid voltage v_s is sensed, delayed by 90° or T/4 and inverted to obtain $V\sin(\omega t+\phi)$ and $-V\cos(\omega t+\phi)$. The VCO output frequency is used to clock a counter which addresses two ROM-DACs with $\sin\theta'$ and $\cos\theta'$ values stored in ROMs.

$$\begin{aligned}\varepsilon_{pd} &= V\sin\left(\omega t+\phi\right)\cos\left(\omega' t+\phi'\right) \\ &\quad - V\cos\left(\omega t+\phi\right)\sin\left(\omega' t+\phi'\right) \\ &= V\sin\left(\left(\omega-\omega'\right)t+\left(\phi-\phi'\right)\right) \\ &= V\sin\left(\theta-\theta'\right)\end{aligned} \tag{6.48}$$

It is clear that the higher frequency term is eliminated, thus there is no requirement for a filter with sharp discrimination between two frequencies which are low and close.

The in-quadrature arrangement of figure 6.20 is similar to stationary $\alpha\beta$ and rotating dq frame transformations (to be covered later) that are used in many power conversion systems. We may write

$$v_s = V\sin\theta = V\sin\left(\omega t+\phi\right) \tag{6.49}$$

The output signals from the quadrature signal generator of Figure 6.20 can be written as

$$\boldsymbol{v}_{(\alpha\beta)} = \begin{bmatrix} v_\alpha \\ v_\beta \end{bmatrix} = V\begin{bmatrix} \sin\theta \\ -\cos\theta \end{bmatrix} \tag{6.50}$$

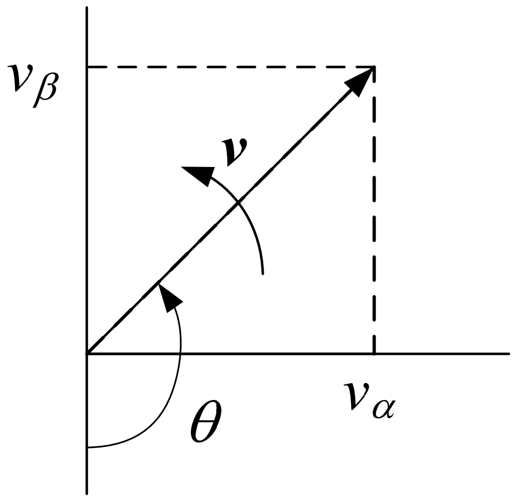

Figure 6.22

The multiplication blocks with *sin*θ*'* and *cos*θ*'* terms imply transformation to a moving frame (*dq*), rotating at ω'. With this transformation,

$$\begin{bmatrix} v_d \\ v_q \end{bmatrix} = \begin{bmatrix} \cos\theta' & \sin\theta' \\ -\sin\theta' & \cos\theta' \end{bmatrix} \begin{bmatrix} v_\alpha \\ v_\beta \end{bmatrix} \tag{6.51}$$

This latter transformation is known as Park transformation, where $\theta'(t) = \int_0^t \omega' dt + \theta_0'$ and ω*'* is the rotational speed in rad/sec of the *dq* axes. Note the transformations of (6.50) and (6.51) are also applied to current I to produce i_α, i_β, and i_d and i_q variables.

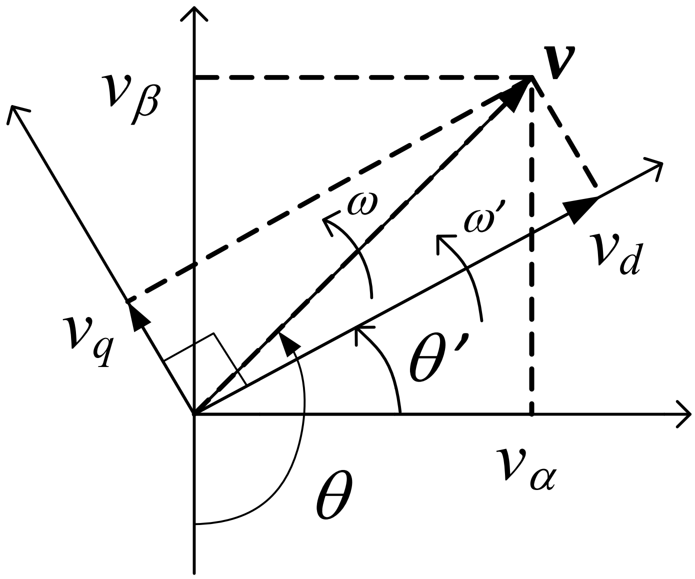

Figure 6.23

When $\omega \approx \omega'$, the voltage vector $\boldsymbol{v}$ and the dq axes will be rotating at the same speed.

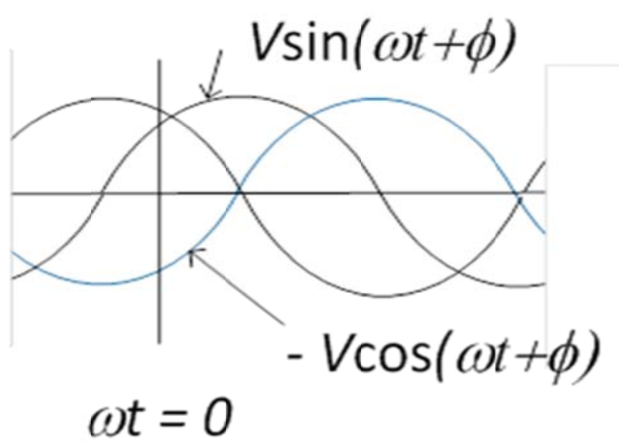

Figure 6.24

When the v_q output from the QSG is connected to the loop PI-filter, as shown in Figure 6.25, and when the PLL is perfectly locked, the d-axis will align with $\boldsymbol{v}$, and $v_q = 0$.

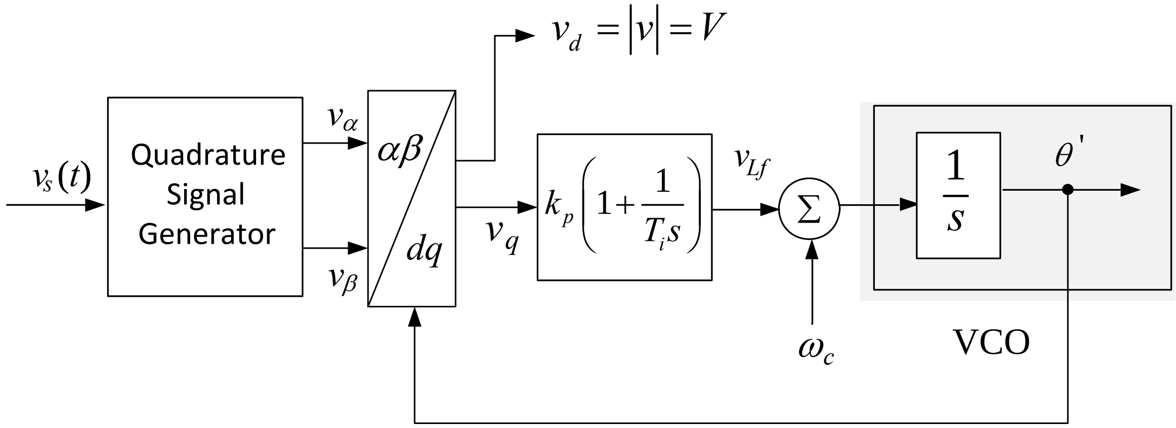

Figure 6.25

In this condition,

$$v_d = |\boldsymbol{v}| = \sqrt{v_d^2 + v_q^2} = V \quad \text{and} \quad \theta' = \theta - \frac{\pi}{2} \qquad (6.52)$$

The response of a PLL with QSG thus does not suffer from bandwidth limitation. This implies that the $\omega + \omega'$ signal is effectively removed from the loop filter. Note that this was assumed in equations 6.37 – 6.47. The response of the PLL with QSG, as indicated in Figure 6.26, now conforms to equations 6.37 - 6.47.

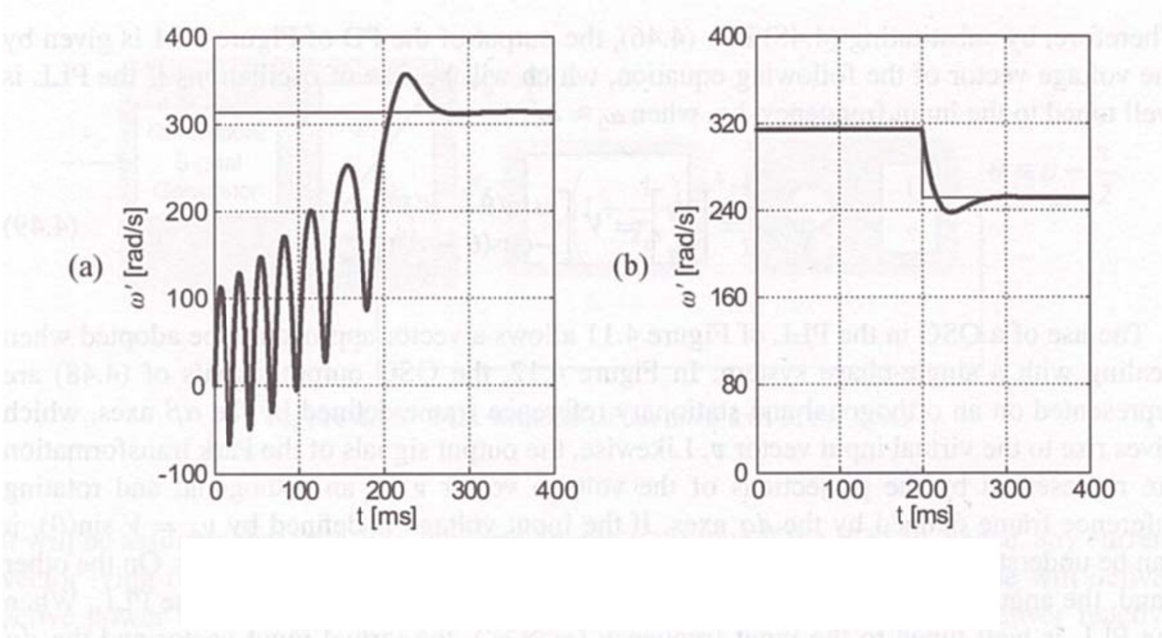

Figure 6.26. QSG PLL response

Angle θ from the PLL can be used to control active and reactive powers, P and Q, from the inverter to the grid. If the inverter output current is placed entirely in the q-axis, i.e., in phase with v_s, only real power is delivered into the grid. By establishing i_d and i_q currents, both active and reactive power is delivered into the grid.

More elaborate PLLs with better frequency tracking and dynamic characteristics are described in Textbook 3. These, however, will not be included in this course. These are left for further reading for those who are interested.

6.4 Voltage, current, active and reactive powers of single-phase systems in synchronous *dq* frame.

With θ obtained from a PLL, voltages and currents in the $\alpha\beta$ reference frame can be transformed to *dq* axes using the Park transformation (see equations 6.50 and 6.51). Control of current, voltage and power are then exercised in the synchronously rotating *dq* reference frame in which variables are at close to zero frequency in the steady state. This simplifies controller designs and delivers faster transient responses.

$$p = \begin{bmatrix} v_d & v_q \end{bmatrix} \begin{bmatrix} i_d \\ i_q \end{bmatrix} = v_d i_d + v_q i_q \qquad (6.53)$$

$$q = v_q i_d - v_d i_q \qquad (6.54)$$

When power references p^* and q^* are specified, current references i_d^* and i_q^* are obtained by solving equations 6.53 and 6.54 with measured v_d and v_q values as coefficients.

The α,β,o voltages and currents in equations (6.50) and (6.51) can be further transformed by using angle

θ', which is obtained by a PLL which synchronizes with voltage v_a.

$$\begin{bmatrix} v_d \\ v_q \end{bmatrix} = \begin{bmatrix} \cos\theta' & \sin\theta' \\ -\sin\theta' & \cos\theta' \end{bmatrix} \begin{bmatrix} v_\alpha \\ v_\beta \end{bmatrix} \tag{6.55}$$

Similarly,

$$\begin{bmatrix} i_d \\ i_q \end{bmatrix} = \begin{bmatrix} \cos\theta' & \sin\theta' \\ -\sin\theta' & \cos\theta' \end{bmatrix} \begin{bmatrix} i_\alpha \\ i_\beta \end{bmatrix} \tag{6.56}$$

Note that measured voltages v_d, v_q and currents i_d and i_q are quadrature variables which rotate at the same frequency as the frequency of v_s, in the synchronously *dq* rotating frame.

Tutorial 3 Problem 3

Power transfer in single-phase systems

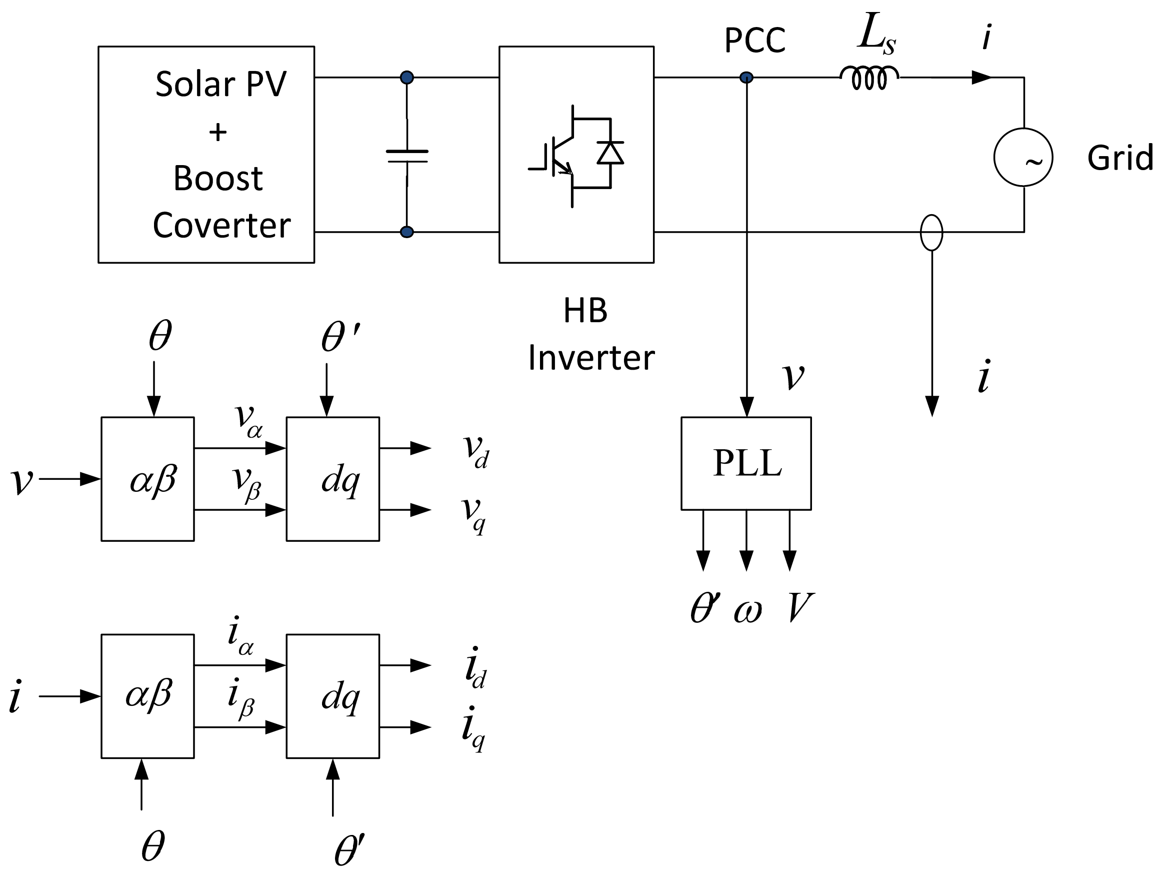

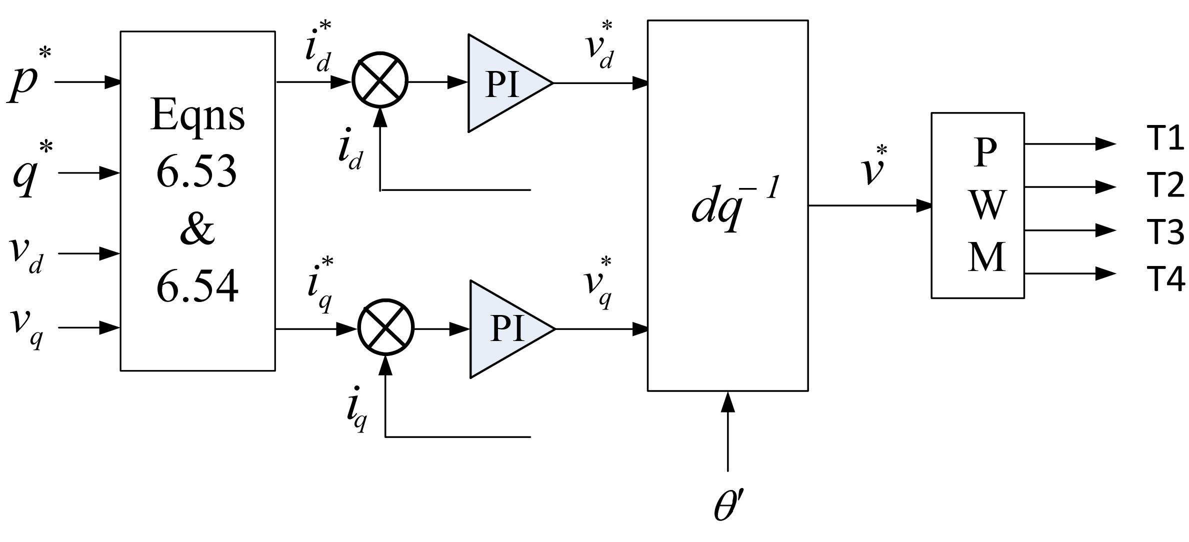

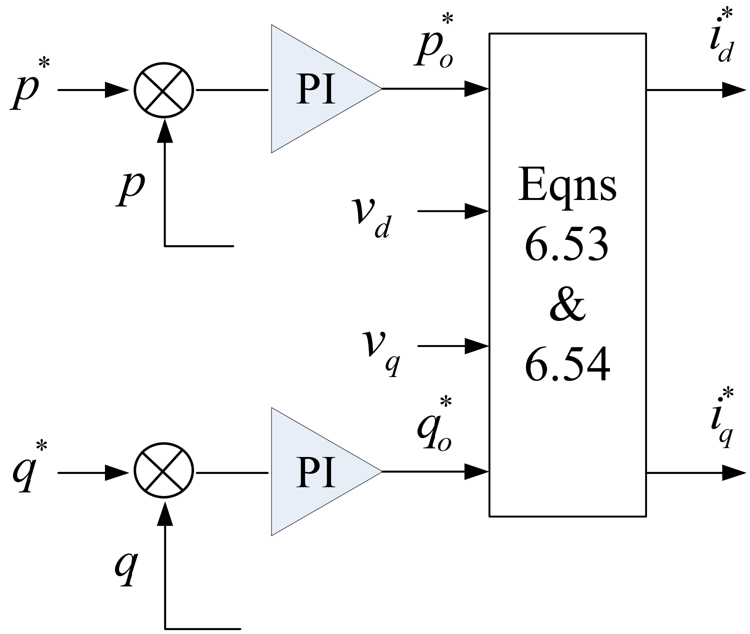

Figure 6.27

6.5 Axes transformation in a three-phase sysem.

6.5.1 Voltage, current, active and reactive powers of a balanced 3-phase systems without harmonic distortion.

$$\boldsymbol{v}_{abc} = \begin{bmatrix} v_a \\ v_b \\ v_c \end{bmatrix} = V \begin{bmatrix} \cos(\omega t + \phi) \\ \cos\left(\omega t - \frac{2\pi}{3} + \phi\right) \\ \cos\left(\omega t - \frac{4\pi}{3} + \phi\right) \end{bmatrix} \qquad (6.57)$$

$$\boldsymbol{v} = \begin{bmatrix} v_a \\ v_b \\ v_c \end{bmatrix} \qquad \boldsymbol{i} = \begin{bmatrix} i_a \\ i_b \\ i_c \end{bmatrix} \qquad (6.58)$$

These voltages are transformed to αβ voltages by the Clarke transformation of (6.59)

$$\begin{bmatrix} v_\alpha \\ v_\beta \\ v_o \end{bmatrix} = \sqrt{\frac{2}{3}} \begin{bmatrix} 1 & -\frac{1}{2} & -\frac{1}{2} \\ 0 & \frac{\sqrt{3}}{2} & -\frac{\sqrt{3}}{2} \\ \frac{1}{\sqrt{2}} & \frac{1}{\sqrt{2}} & \frac{1}{\sqrt{2}} \end{bmatrix} \begin{bmatrix} v_a \\ v_b \\ v_c \end{bmatrix} \qquad (6.59)$$

Similarly i_a, i_b, i_c are transformed to i_α, i_β and i_o.

$$\begin{bmatrix} i_\alpha \\ i_\beta \\ i_o \end{bmatrix} = \sqrt{\frac{2}{3}} \begin{bmatrix} 1 & -\frac{1}{2} & -\frac{1}{2} \\ 0 & \frac{\sqrt{3}}{2} & -\frac{\sqrt{3}}{2} \\ \frac{1}{\sqrt{2}} & \frac{1}{\sqrt{2}} & \frac{1}{\sqrt{2}} \end{bmatrix} \begin{bmatrix} i_a \\ i_b \\ i_c \end{bmatrix} \qquad (6.60)$$

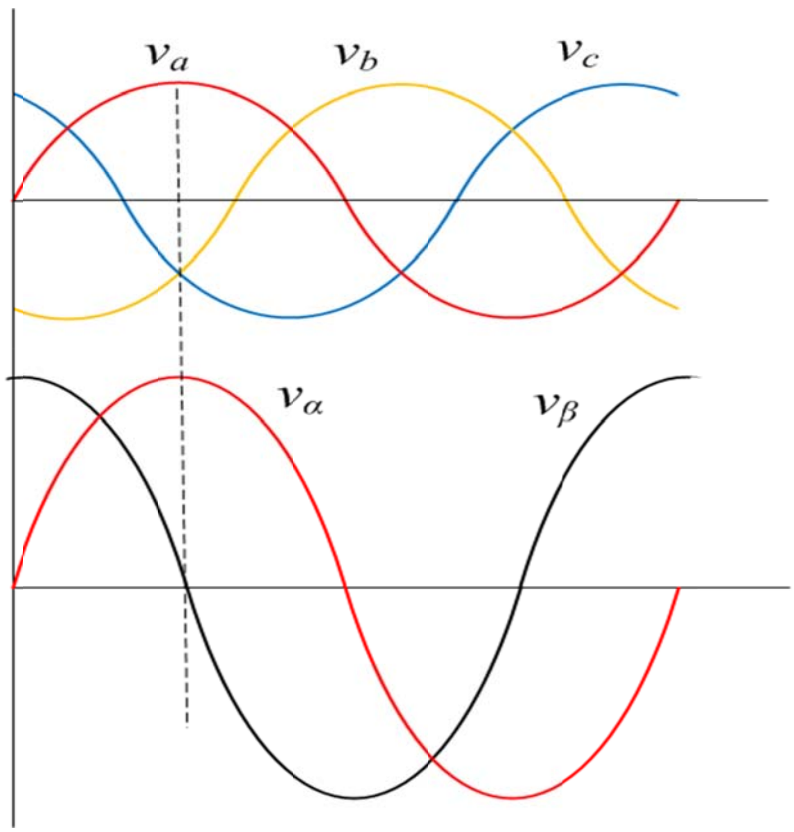

Figure 6.28

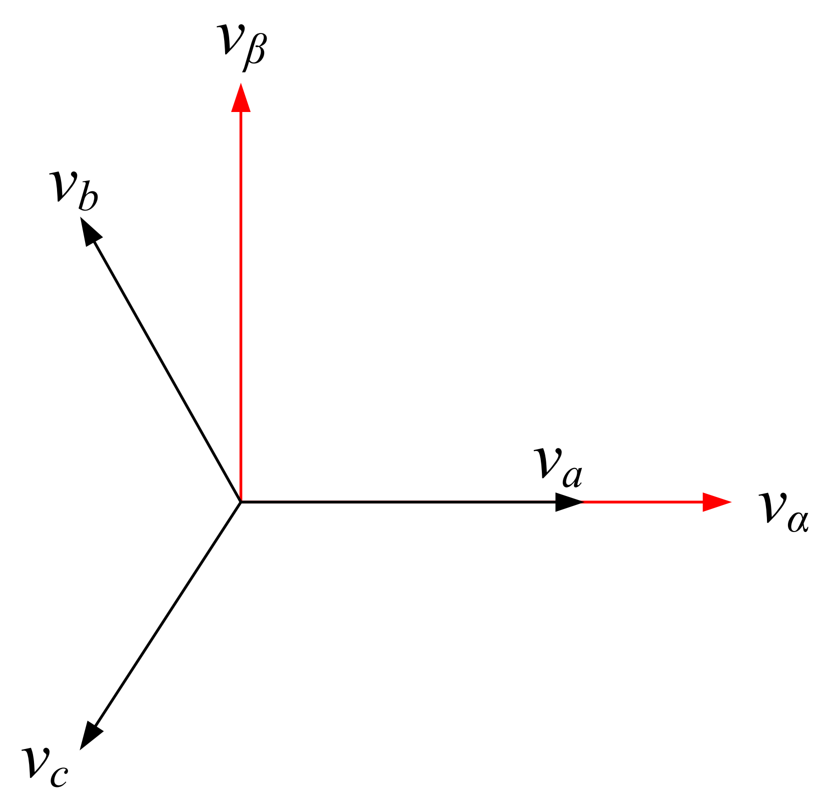

Figure 6.29 v_{abc} and $v_{\infty\beta}$ voltage phasors.

With this transformation, $v_\alpha^2 + v_\beta^2 + v_o^2 = v_a^2 + v_b^2 + v_c^2$. (power invariant) and,

$$\sqrt{v_\alpha^2 + v_\beta^2 + v_o^2} = \sqrt{v_a^2 + v_b^2 + v_c^2} = \sqrt{\frac{3}{2}}V \qquad (6.61)$$

With this transformation, power remains invariant.

$$p = v_{\alpha\beta o} \bullet i_{\alpha\beta o} = v_{abc} \bullet i_{abc} \qquad (6.62)$$

$$p = p = \begin{bmatrix} v_\alpha & v_\beta & v_o \end{bmatrix} \begin{bmatrix} i_\alpha \\ i_\beta \\ i_o \end{bmatrix} = \begin{bmatrix} v_a & v_b & v_c \end{bmatrix} \begin{bmatrix} i_a \\ i_b \\ i_c \end{bmatrix} \tag{6.63}$$

A different form of Clarke transformation is:

$$\begin{bmatrix} v_\alpha \\ v_\beta \\ v_o \end{bmatrix} = \frac{2}{3} \begin{bmatrix} 1 & -\frac{1}{2} & -\frac{1}{2} \\ 0 & \frac{\sqrt{3}}{2} & -\frac{\sqrt{3}}{2} \\ \frac{1}{\sqrt{2}} & \frac{1}{\sqrt{2}} & \frac{1}{\sqrt{2}} \end{bmatrix} \begin{bmatrix} v_a \\ v_b \\ v_c \end{bmatrix} \tag{6.64}$$

$$\begin{bmatrix} i_\alpha \\ i_\beta \\ i_o \end{bmatrix} = \frac{2}{3} \begin{bmatrix} 1 & -\frac{1}{2} & -\frac{1}{2} \\ 0 & \frac{\sqrt{3}}{2} & -\frac{\sqrt{3}}{2} \\ \frac{1}{\sqrt{2}} & \frac{1}{\sqrt{2}} & \frac{1}{\sqrt{2}} \end{bmatrix} \begin{bmatrix} i_a \\ i_b \\ i_c \end{bmatrix} \tag{6.65}$$

With this transformation, the power does not remain invariant; however, the amplitudes of $\alpha\beta o$ quantities remain the same as for *abc* quantities. This is helpful in simulation and measurement, because the same amplitudes of voltages and currents produce important checkpoints. With this transformation

$$p = \frac{3}{2}\begin{bmatrix} v_\alpha & v_\beta & v_o \end{bmatrix}\begin{bmatrix} i_\alpha \\ i_\beta \\ i_o \end{bmatrix} = \begin{bmatrix} v_a & v_b & v_c \end{bmatrix}\begin{bmatrix} i_a \\ i_b \\ i_c \end{bmatrix} \qquad (6.66)$$

The Clarke transformations of (6.64 – 6.66) are thus adopted henceforth.

6.5.2 Transformation to *dqo* frame

Transformations of $\alpha\beta o$ quantities to dqo quantities in the synchronously rotating dqo frame is given by Park transformation

$$\begin{bmatrix} v_d \\ v_q \\ o \end{bmatrix} = \begin{bmatrix} \cos\theta & \sin\theta & 0 \\ -\sin\theta & \cos\theta & 0 \\ 0 & 0 & 1 \end{bmatrix} \begin{bmatrix} v_\alpha \\ v_\beta \\ v_o \end{bmatrix} \qquad (6.67)$$

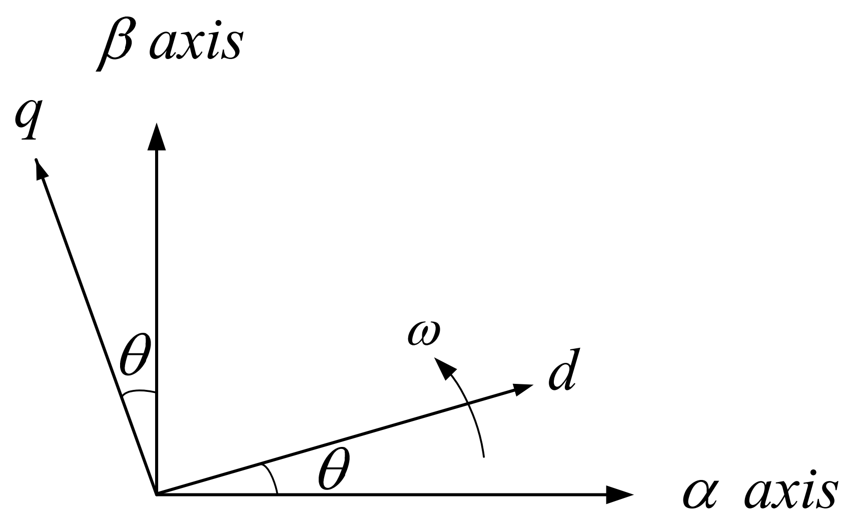

Figure 6.30 Stationary $\alpha\beta$ and synchronously rotating dq axes.

Note that transformation matrices of (6.64) (or (6.65)) and (6.67) can be multiplied to obtain a composite transformation given by (6.68).

$$\begin{bmatrix} v_d \\ v_q \\ o \end{bmatrix} = \frac{2}{3}\begin{bmatrix} \cos\theta & \cos\left(\theta-\frac{2\pi}{3}\right) & \cos\left(\theta-\frac{4\pi}{3}\right) \\ -\sin\theta & -\sin\left(\theta-\frac{2\pi}{3}\right) & -\sin\left(\theta-\frac{4\pi}{3}\right) \\ \frac{1}{\sqrt{2}} & \frac{1}{\sqrt{2}} & \frac{1}{\sqrt{2}} \end{bmatrix}\begin{bmatrix} v_a \\ v_b \\ v_o \end{bmatrix}$$

(6.68)

The active (real) and reactive power equations in the *dq* reference frame with the transformations of (6.64) and (6.67) or (6.68) are

Active power, $p = \frac{3}{2}\left(v_d i_d + v_q i_q\right)$ W (6.69)

Reactive power, $q = \frac{3}{2}\left(v_q i_d - v_d i_q\right)$ W (6.70)

6.4.3 The instantaneous *pq* theory

$$\begin{bmatrix} p_{\alpha\beta} \\ q_{\alpha\beta} \\ p_o \end{bmatrix} = \begin{bmatrix} v_\alpha & v_\beta & 0 \\ -v_\beta & v_\alpha & 0 \\ 0 & 0 & v_o \end{bmatrix} \begin{bmatrix} i_\alpha \\ i_\beta \\ i_o \end{bmatrix} \tag{6.71}$$

where $$\left[M_{\alpha\beta o}\right] = \begin{bmatrix} v_\alpha & v_\beta & 0 \\ -v_\beta & v_\alpha & 0 \\ 0 & 0 & v_o \end{bmatrix} \tag{6.72}$$

$p_{\alpha\beta}$ = instantaneous real/active power, W

$q_{\alpha\beta}$ = instantaneous imaginary/reactive power, W

p_o = instantaneous zero-sequence power, W

$$p_{\alpha\beta} = \frac{3}{2}\left(v_\alpha i_\alpha + v_\beta i_\beta + v_o i_o\right) = v_a i_a + v_b i_b + v_c i_c \tag{6.73}$$

$$= \frac{3}{2}\left(v_d i_d + v_q i_q\right) \tag{6.74}$$

$$q_{\alpha\beta} = \frac{3}{2}\left(v_\alpha i_\beta - v_\beta i_\alpha\right) \tag{6.75}$$

$$= \frac{3}{2}\left(v_q i_d - v_d i_q\right) \tag{6.76}$$

$$p_o = \frac{3}{2} v_o i_o = 0 \text{ for a balanced system.} \qquad (6.77)$$

Equations (6.74) and (6.76) can be used for obtaining both power feedback from measured v_{dq} and i_{dq} quantities and for obtaining d and q axes current references i_d^* and i_q^*, when references for active and reactive powers, p^* and q^* are available.

$$\left[M_{\alpha\beta o}\right]^{-1} = \frac{1}{v_a^2 + v_\beta^2} \begin{bmatrix} v_\alpha & -v_\beta & 0 \\ v_\beta & v_\alpha & 0 \\ 0 & 0 & 1/v_o \end{bmatrix} \qquad (6.81)$$

When power references $p_{\alpha\beta}^*, q_{\alpha\beta}^*$, and p_o^* are available

$$i_{\alpha\beta o}^* = \left[M_{\alpha\beta o}\right]^{-1} \begin{bmatrix} p_{\alpha\beta}^* \\ q_{\alpha\beta o}^* \\ p_o^* \end{bmatrix} \qquad (6.82)$$

$$i_{\alpha\beta}^* = \begin{bmatrix} i_\alpha^* \\ i_\beta^* \end{bmatrix} = \frac{1}{v_\alpha^2 + v_b^2} \begin{bmatrix} v_\alpha & -v_\beta \\ v_\beta & v_\alpha \end{bmatrix} \begin{bmatrix} p_{\alpha\beta}^* \\ q_{\alpha\beta o}^* \end{bmatrix} \qquad (6.83)$$

Note that i_α^* and i_β^* are sinusoidal references. Controlling i_α *and* i_β to control powers p and q suffers from following error due to these time varying signals. A faster and more accurate approach is the control scheme for active and reactive power control in the synchronously rotating dq reference frame is indicated in figure 6.31. In this reference frame, all dq variable are at close zero frequency when the PLL tracks v_s closely.

Voltages and currents at the PCC are transformed into $\alpha\beta$ and dq frames first. The PLL synchronizes v_a and obtains the angle θ of the voltage v_a at the PCC.

References i_d^* and i_q^* are obtained from the active and reactive power references and equations 6.74 and 6.76. These are to be regulated continuously, say by proportional + integral (PI) controllers.

The i_d and i_q current regulators, norally PI regulators, produce voltage references v_{di}^* and v_{qi}^* in the dq reference frame for the inverter. These are re-transformed back into references v_a^*, v_b^* and v_c^* for the PWM modulator for the inverter (see Figure 6.31) using equation 6.68.

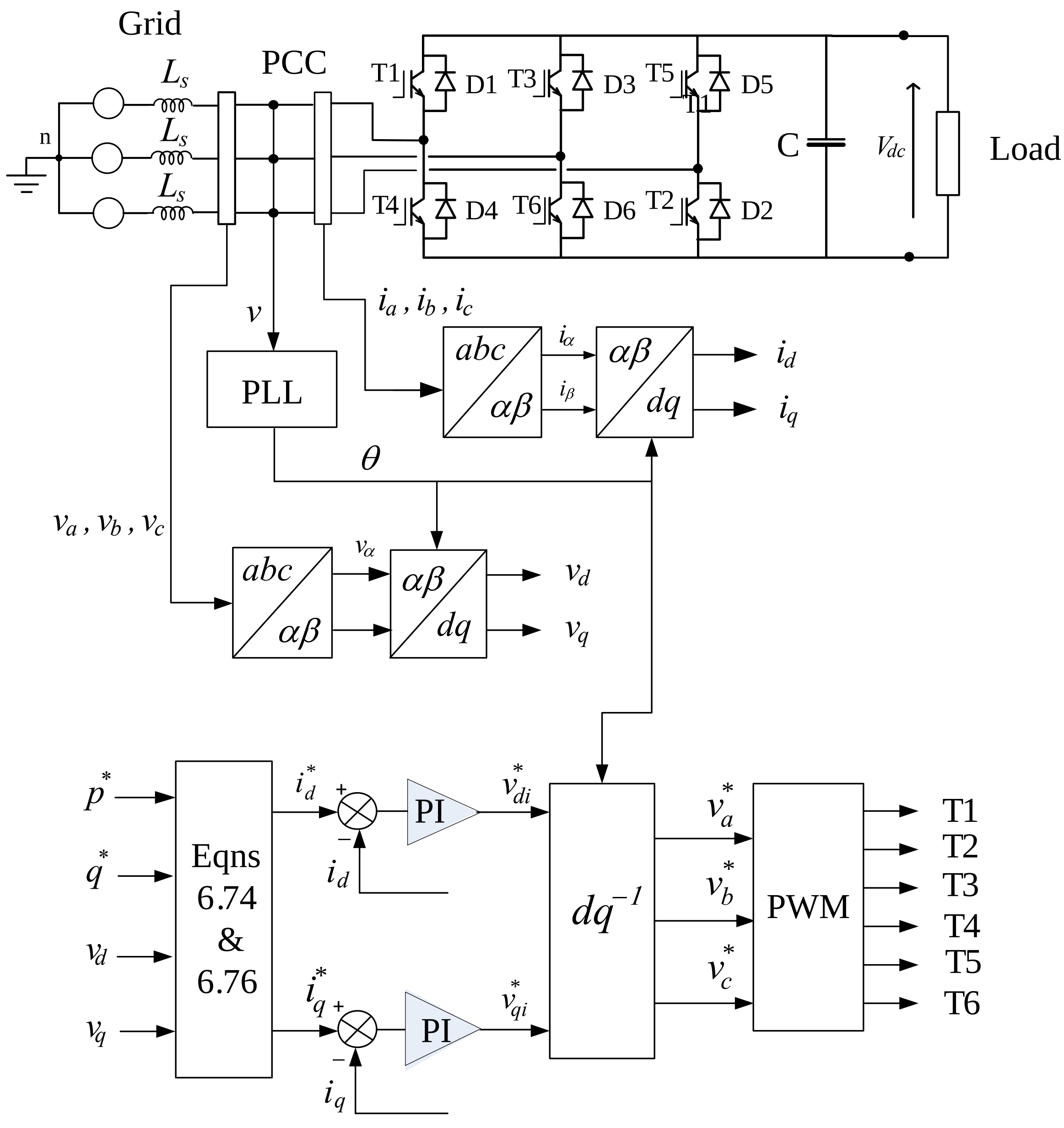

Figure 6.31

Note that the above analyses have neglected harmonics and unbalance in the measured variables v_{abc} and i_{abc} at the PCC. With these assumptions, and when the inverter operates at a frequency which is close to the frequency of the grid at steady-state, all voltage and current variables in the *dq* reference frame are virtually DC quantities.

When power is supplied from the AC grid to a DC source, for charging a battery or for supplying power to a DC grid and DC loads, there is an additional requirement to maintain the DC output voltage to a constant specified value. This DC voltage must be higher than the peak line-line voltage of the AC grid, because of the boost conversion used. In such cases, there is a voltage controller for regulating the DC output voltage to a reference V_{DC}^*. This followed by i_d and i_q current controllers in Figure 6.31.